Implementation of glass-curtain-wall cleaning robot driven by double flexible rope

Article *in* Industrial Robot · August 2014

DOI: 10.1108/IR-01-2014-0303

Industrial Robot: An International Journal

Implementation of glass-curtain-wall cleaning robot driven by double flexible rope

Jiang Jin-gang Zhang Yong-de Zhang Shu

Implementation of glass-curtain-wall cleaning robot driven by double flexible rope

Jiang Jin-gang and Zhang Yong-de
Intelligent Machine Institute, Harbin University of Science and Technology, Harbin, China, and
Zhang Shu
College of Seeking, Zhejiang University, Hangzhou, China

Abstract

Purpose – The purpose of this paper is to implement a glass-curtain-wall cleaning robot driven by a double flexible rope, so as to replace manual cleaning. The glass-curtain-wall, because of its excellent daylighting performance, damp-proofing characteristics, heat insulation properties and aesthetics, is widely used in modern city buildings. For glass-curtain-wall buildings, regular cleaning of the glass-curtain-wall is necessary to ensure that the surface of the building appears clean and tidy, which in turn contributes toward preserving the overall aesthetic appearance of the city. Currently, the primary method of cleaning glass curtain walls is manual cleaning by workers on a suspended platform.

Design/methodology/approach – The mechanical structure of the proposed glass-curtain-wall cleaning robot driven by a double flexible rope is inspired by the way a spider moves by pulling its silk draglines in the air. For self-locking protection and increased rope friction, the robot's moving section includes a worm reducer and multislot master–slave roller. The cleaning section comprises a water tank, control valve, shower nozzle and brush. The wall adsorbing section is realized by a double rotor. The workspace of the robot is analyzed. Flexible rope winding and unreeling control of the cleaning robot is deduced. The force of the cleaning robot when the double rotor is working is analyzed and calculated. The prototype of the glass-curtain-wall cleaning robot model driven by a double flexible rope is established, and experiments wherein the robot moves along a preset track, as well as cleaning experiments, are performed.

Findings – The prototype of the glass-curtain-wall cleaning robot model driven by a double flexible rope can move along the preset track, satisfy the design functions and clean effectively. The experimental results verify the validity and practicality of the robot.

Research limitations/implications – The implication of this research is that a glass-curtain-wall cleaning robot model driven by a double flexible rope fulfills the movement strategy and drive-type requirements for cleaning glass curtain walls. The limitation of this research is that it is difficult to implement rapid cleaning.

Originality/value – The traditional method of manual cleaning by workers on a suspended platform will be changed after the glass-curtain-wall cleaning robot is manufactured, and the advent of this cleaning robot for the low- and mid-rise buildings will reduce the cost of cleaning buildings, improve the working environment and enhance production efficiency.

Keywords Glass-curtain-wall cleaning robot, Double flexible rope, Workspace analysis, Motion analysis, Force analysis

Paper type Research paper

1. Introduction

The glass curtain wall, because of its excellent daylighting performance, damp-proofing characteristics, heat insulation properties and aesthetics, is widely used in modern city buildings. Glass-curtain-wall buildings contribute significantly to the aesthetic appearance of the modern city (Akinfiev *et al.*, 2009; Zhang and Wang, 2010; Qian *et al.*, 2006; Chu *et al.*, 2010). Thus, regular cleaning of the glass curtain walls of buildings is necessary not only for maintaining the clean and tidy external appearance of individual buildings but also for preserving the overall aesthetic appearance of the city. At present, the primary method of cleaning glass curtain walls is manual cleaning by workers on a suspended platform. This method is totally dependent on manual work and suffers from shortcomings such as high labor intensity, low efficiency and high risk (Zhang *et al.*, 2006; Zhao *et al.*, 2004; Xu *et al.*, 2011; Kalra and Gu, 2007). Every year, most of the reported injuries and deaths in the field of cleaning of buildings are caused by this work, which makes it the biggest hidden danger to the personal safety of the workers (Guido *et al.*, 2002; Zhu *et al.*, 2003, 2002; Sun *et al.*, 2004; Schmidt and Berns, 2013). Therefore, the growth in the construction of glass-curtain-wall buildings must be accompanied by the development of a robot that can replace the manual labor involved in the cleaning of glass curtain walls.

Since the 1990s, researchers from Japan have taken the lead in focusing on the automated cleaning method, and the

The current issue and full text archive of this journal is available at
www.emeraldinsight.com/0143-991X.htm

Industrial Robot: An International Journal
41/5 (2014) 429–438

[DOI 10.1108/IR-01-2014-0303]

The authors are extremely grateful to the anonymous referees for their most insightful and constructive comments, which have enabled them to improve the manuscript significantly. The authors are also grateful to the Editor-in-Chief and the technical editor for reviewing and editing the paper. This research was supported by the National Natural Science Foundation of China (Grant No. 51205093), the Heilongjiang Province Education Bureau Project (Grant No. 12541147) and the Key Research Project Post-graduate Innovation Foundation of Heilongjiang Province (Grant No. YJSCX2011-004HLJ).

Industrial Robot: An International Journal
Volume 41 · Number 5 · 2014 · 429–438

glass-curtain-wall cleaning robot has come into being. At present, techniques and applications of glass-curtain-wall cleaning robots are an active research area, and many studies at scientific research institutions have made significant achievements (Hwang *et al.*, 2008; Tavakoli *et al.*, 2013; Lee *et al.*, 2012). Single- and multi-suction cup-type robots for cleaning outer walls of high-rise buildings have been studied (Chen and Yeo, 2003; Menon and Metin, 2006; Liu *et al.*, 2006), in addition to crawler-type wall cleaning robot. Sameoto *et al.* (2008), Guan *et al.* (2013) and Wang *et al.* (2010) studied a bionic wall moving cleaning robot, and the adhesion and structural types based on bionic theory have been studied (He *et al.*, 2014; Hu *et al.*, 2009; Jaradat *et al.*, 2010; Suzuki *et al.*, 2010). The adsorption type, vacuum adsorption force, traction force and wall adaptive capacity of a wall cleaning robot have been analyzed (Qian *et al.*, 2006; Yu *et al.*, 2011; Hirai *et al.*, 2013; Koo *et al.*, 2013). The movement form of the above-mentioned robot primarily depends on the vehicle wheel, crawler and walking mechanism (two-leg or multi-leg).

In this paper, a type of bionic wall climbing cleaning robot inspired by spiders that move in the air is presented. Non-contact motion of the robot on the wall is realized by coordinating the winding and unreeling of two flexible ropes. The robot's adsorption on the wall is realized by the thrust generated by the double rotor. This type of safe, reliable, lightweight, high-efficiency and high performance-to-price ratio cleaning robot will undoubtedly be highly competitive on the market. The advent of a cleaning robot for low- and mid-rise buildings will reduce the cost of cleaning buildings, improve the working environment, enhance production efficiency and promote the development of the cleaning domain tremendously. In addition, it has positive social benefits, economic significance and the prospect of wide application.

2. Overall scheme design of glass-curtain-wall cleaning robot driven by double flexible rope

Three functions are needed for the glass-curtain-wall cleaning robot to move freely on the wall and accomplish certain functions. These are the moving, adsorption and cleaning functions. A double flexible rope, located at two sides of the robot, is adopted to drive the robot. Two flexible ropes are driven by two DC motors independently. To increase the friction force of the rope, two sets of rollers with multiple slots, which effectively increase the friction force, are designed. A potentiometer is used to detect the deflection angle of the ropes. A horizontally oriented slider is designed to adapt to the horizontal position change of the potentiometer and its holder. The thrust generated by the double rotors accomplishes the adsorption of the robot on the wall, and simultaneously creates positive pressure on the brush for cleaning. The spray of the cleaning fluid is accomplished by the combination of the water tank, control valve and shower nozzle, and the wall cleaning function is finished by the two motor-driven revolving brushes. The robot is controlled by SPCE061A, and wireless control is realized by the Bluetooth module.

The total area of the experimental platform is 1000 mm × 2000 mm, and it is used as a cleaning platform. The overall structure of the glass-curtain-wall cleaning robot consists of an oriented slider, rotor, DC motor, fixed holder, water pump, water tank, cleaning brush and many kinds of fasteners. The overall structure of the glass-curtain-wall cleaning robot driven by a double flexible rope is shown in Figure 1 and Figure 2.

3. Structure design of glass-curtain-wall cleaning robot

3.1 Structure of the roller set

3.1.1 Wrap mode of the flexible rope

The robot is driven by two flexible ropes that are fixed above the curtain walls of the building. The other sides of the two ropes twine around the two stagger rollers. The master roller is driven by a DC motor, and the robot's movement on the XY plane of the curtain wall is accomplished through coordinated control of the winding and unreeling of two flexible ropes. The robot's movement is controlled by the two flexible ropes, and the tangency point between the flexible rope and the roller is the point that bears the whole force of the robot. Changing this point will make a difference to the force-bearing condition of the robot. Because the winding and unreeling of the flexible rope is realized by the friction between the rope and the roller, the type and precision of the movement are determined by the twining method of the rope.

If one roller is used, the slot profile is continuous screw type, and the flexible rope is twined in the slot. When the roller rotates, the flexible rope twines along the slot due to the friction of the inner wall of the slot. This scheme can accomplish the winding and unreeling of the flexible rope. However, the flexible rope tight side point changes in the circumferential and axial directions of the roller. This is detrimental to the force balance of the robot, and the length of the track imposes a restriction on the length that the flexible rope can wind and unreel. When two rollers with multiple slots are used cooperatively, with master roller above the slave roller, the flexible rope twines from the first slot of the master roller to the first slot of the slave roller, and then twines from the first slot on the slave roller to the second slot on the master

Figure 1 Overall structure of glass-curtain-wall cleaning robot driven by a double flexible rope: front view of cleaning robot

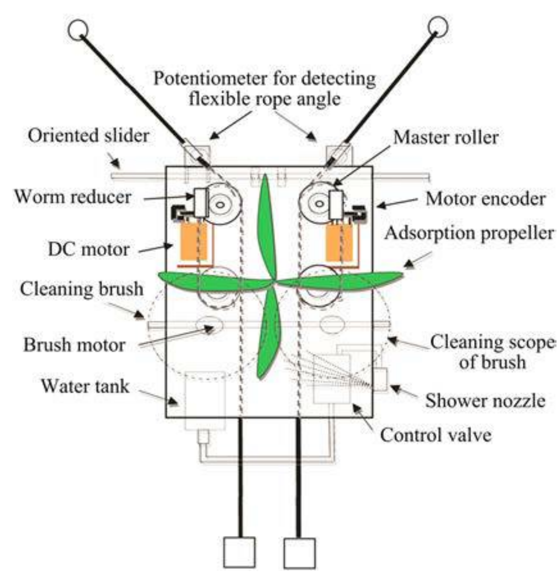

Figure 2 Overall structure of glass-curtain-wall cleaning robot driven by a double flexible rope: left view of cleaning robot

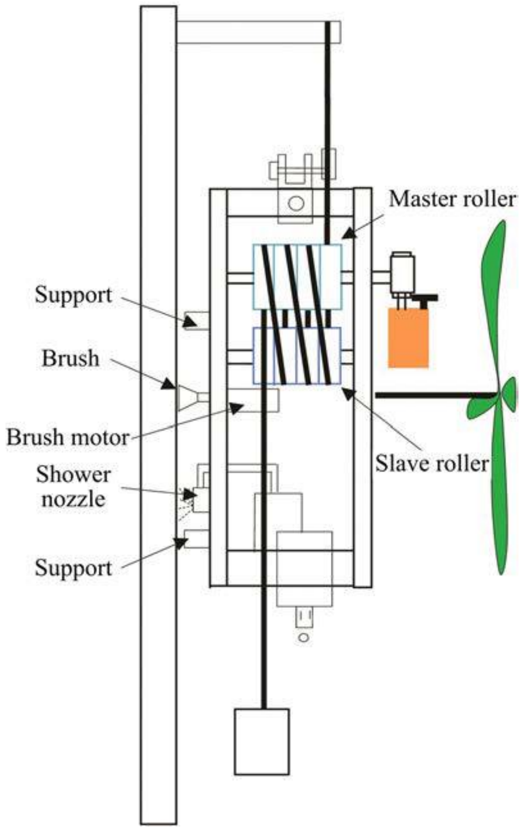

roller. As shown in Figure 3, the screw is formed through this orderly twining. This method can guarantee that the flexible rope tight side point on the master roller does not change in the axial direction of the roller, so that the force balance of the robot can be adjusted easily, and the number of the slots does not impose a restriction on the length that the flexible rope can wind and unreel. In other words, the number of the slot does not restrict the reachable workspace of the robot.

3.1.2 Slot number of the roller

Taking the DC motor of the right flexible rope and four slots as an example, the force analysis is as shown in Figure 4, and the friction on the slave shaft can be neglected. The tensile force on section 1 is F, the tensile force on section 2 and 3 is f_1, the tensile force on section 4 and 5 is f_2, the tensile force on section 6 and 7 is f_3 and the tensile force on section 8 is $f_4 = mg$. The frictions of slot a, b, c and d are $f_{\mu a}$, $f_{\mu b}$, $f_{\mu c}$, and $f_{\mu d}$, respectively, so:,

$$\begin{cases} F = f_1 + f_{\mu a} \\ f_1 = f_2 + f_{\mu b} \\ f_2 = f_3 + f_{\mu c} \\ f_3 = f_4 + f_{\mu d} \\ f_4 = mg \end{cases} \tag{1}$$

$$\Rightarrow F = f_{\mu a} + f_{\mu b} + f_{\mu c} + f_{\mu d} + mg \tag{2}$$

Let

$$\sum f_\mu = f_{\mu a} + f_{\mu b} + f_{\mu c} + f_{\mu d} \tag{3}$$

Figure 3 Winding mode of double roll flexible rope

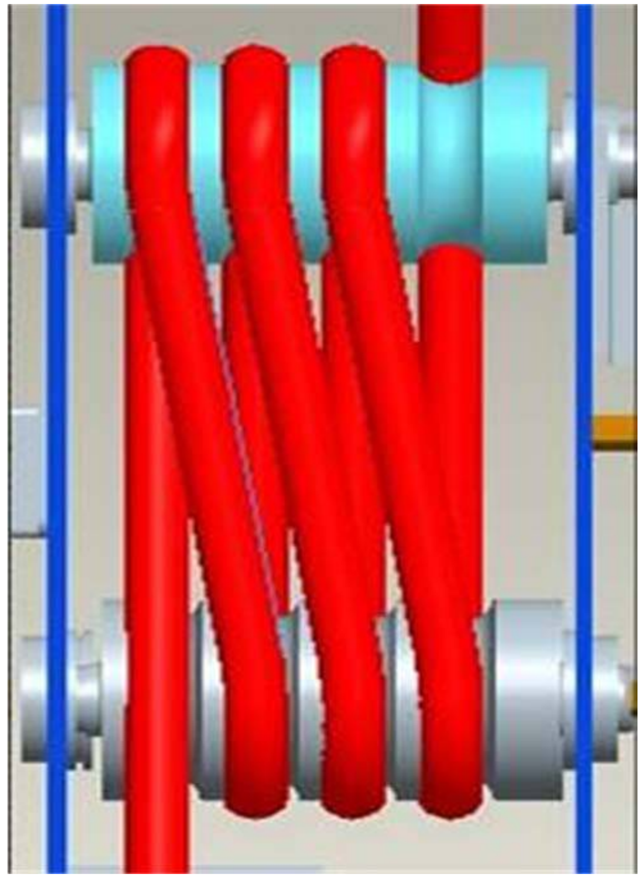

$$\Rightarrow \sum f_\mu = F - mg \tag{4}$$

Because the weight per meter of the flexible rope is very small, and the movement speed of the flexible rope is low, we can neglect the influence of the centrifugal force. When the flexible rope is at the slipped critical state, the tight side tension F and slack side tension f meet the Euler equation of the flexible body friction:

Figure 4 Force analysis of "0" type winding mode

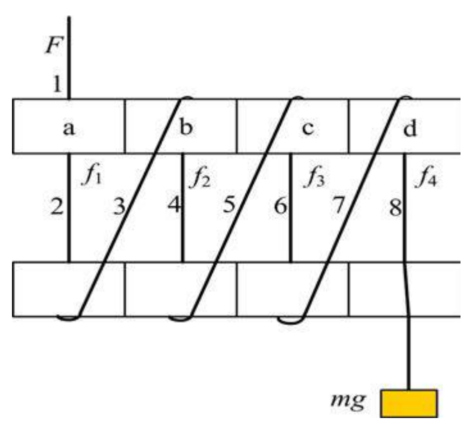

$$F/f = e^{\mu\alpha} \tag{5}$$

Where α is the central angle of the contact arc of the belt and pulley, which is named the wrap angle. μ is the friction coefficient.

The effective tension force on each slot of the roller is equal to the friction that the flexible rope bears on the slot of the roller. Therefore, the maximum effective tension force F_{max} that the flexible rope can transmit is:

$$F_{\max} = F - f = F(1 - \frac{1}{e^{\mu\alpha}}) = f(e^{\mu\alpha} - 1) \tag{6}$$

Thus, the maximum friction is mainly dependent on the friction coefficient, the wrap angle and the tension force of the belt. When the flexible rope slips, every section of the rope is at the state that transmits the maximum effective tension force. Therefore:

$$\begin{cases} f_{\mu a} = f_1(e^{\mu\alpha 1} - 1) \\ f_{\mu b} = f_2(e^{\mu\alpha 2} - 1) \\ f_{\mu c} = f_3(e^{\mu\alpha 3} - 1) \\ f_{\mu d} = f_4(e^{\mu\alpha 4} - 1) \end{cases} \tag{7}$$

When the robot is located at the right limit position, the rope remains at the 90° position. At this time α_1 is equal to the deflection angle of the robot. It can be calculated, and is 20°; $\mu = 0.5$. We can then calculate that $f_3 = 5.81\ mg$, $f_2 = 27.95\ mg$, $f_1 = 134.44\ mg$ and $F = 5{,}160.15$N. When $F = G$, the counter weight is $m = M/160.15$, and the weight of the whole robot is 1.8 kg, so the counter weight should be heavier than 11.24 g to ensure that the flexible rope does not slip. Using the same analysis method, and comparing the counter weight, roller size and weight for different numbers of slots, the roller with four slots is found to be the best choice.

3.2 Cleaning section

At present, the method for cleaning glass curtain walls is to spray water on the curtain, and then apply a cleaning cloth. The spraying part consists of a water tank, vacuum pump, atomizer and water pipe. The nozzle of the sprayer is very small. On the basis of the Bernoulli equation, when the water comes out, the pressure increases. The water flow is transformed into spray, and is sprayed onto the glass curtain wall uniformly. This can save the energy and water. A better cleaning effect can be achieved by using a rolling cleaning brush driven by a DC motor.

3.3 Deflection angle detection mechanism of flexible rope

According to the movement relationship of the robot driven by two flexible ropes, only the deflection angles of the two flexible ropes are given in real time. The movement relationship of the optimal position in each direction can be calculated, and the control value of winding and unreeling the flexible rope of the cleaning robot can be obtained. A potentiometer is used to detect the deflection angle of the ropes. A horizontally oriented slider is designed to adapt to the horizontal position change of the potentiometer and its holder. Deflection angle detection mechanism is as shown in Figure 5. It consists of a slider holder, potentiometer, potentiometer holder, oriented slider and oriented sleeve.

Figure 5 Deflection angle detection mechanism of flexible rope

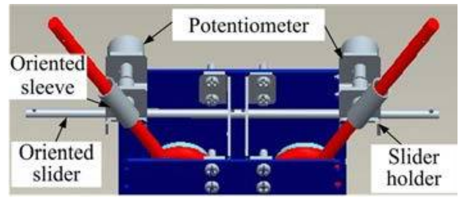

4. Workspace of glass-curtain-wall cleaning robot

According to the flexible rope's horizontal angle γ, β and the span between the two flexible ropes, the limit position of the robot can be determined.

In the horizontal direction, when the left flexible rope stays at the vertical state and the right one stays at the maximum loose state, the robot is located at the left limit position. In this situation, the drive of the right roller DC motor does not work for displacement in the horizontal direction. Similarly, when the right flexible rope stays at the vertical state, the left one remains in a loose state and does not generate tension force. Therefore, the robot can reach the limit position of the experimental platform in the horizontal direction. However, because only one rope generates tension force, this will enable robot deflection in the direction of movement, which is not suitable for cleaning work. Thus, the limit condition should be avoided.

In the horizontal direction, when the robot is located at the left or right limit positions, the robot can reach the maximum height, and can rise to the top height in the horizontal direction. The lowest position that the robot can reach is determined by the length of the rope. If the length of the rope, l , is given, it can reach the downward position $H = \sqrt{[l-4(\pi d+2l_1)]^2-1000^2}$, where d is the diameter of the roller, and l_1 is the vertical length of the inner tangent line between the driving roller and the driven roller.

Due to the limited motor output power, the robot has a movement position limit. When the robot is located at the midperpendicular of the fixed point of the two flexible ropes, $F_1 = F_2$, and $\beta = \gamma$. This gives $2F_1\sin\gamma = Mg$. The loading torque of the roller drive motor is $T_L = 2RF\cos\gamma$. When the robot moves upwards, γ decreases constantly, and the driving torque T increases progressively. When the torque reaches a limit value $T \geq T_L$, the robot reaches the upper-limit position of the midperpendicular.

Suppose that the vertical distance from the central point of the DC motor to the fixed point of the flexible rope is h, the distance from the central point of the DC motor to the left fixed point is s_1, and the distance to the right fixed point is s_2. Then h can be described as follows:

$$h = s_1\tan\gamma = s_2\tan\beta \tag{8}$$

Then,

$$s = s_1 + s_2 = h(\tan^{-1}\gamma + \tan^{-1}\beta) \tag{9}$$

Figure 6 Workspace of the robot

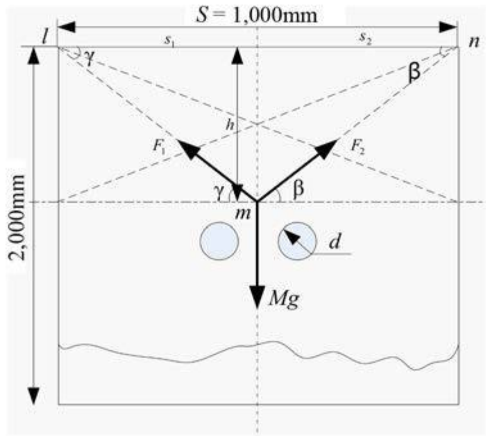

$$F_1 \sin\gamma + F_2 \sin\beta = Mg \tag{10}$$

Where F_1 and F_2 are the tension forces on the left and right flexible ropes, and R is the radius of the roller.

According to the load torque equation, without the rotor working, and with the maximum output torque of the DC motor, the angle of the flexible rope can be calculated:

$$\begin{cases} T_{L1} = \dfrac{(Mg + Ma)R}{(\sin\gamma + \cos\gamma\tan\beta)\eta_c i} \\ T_{L2} = \dfrac{(Mg + Ma)R}{(\sin\beta + \cos\beta\tan\gamma)\eta_c i} \end{cases} \tag{11}$$

The maximum output torque of the motor is $T = 18N{\cdot}mm$. Under maximum torque, the angle of the flexible rope is 20°, and $h = 255$ mm. The segments lm and mn form the upper-limit movement trajectory of the robot. If the rope is long enough, the area below lm and mn is part of the reachable area of the robot. The workspace of the robot is shown in Figure 6.

5. Flexible rope winding and unreeling analysis of cleaning robot

5.1 Robot movement in the horizontal direction

As shown in Figure 7, the robot moves a distance ΔX horizontally toward the right, from the outline of the full line

Figure 7 Moving horizontally from left to right

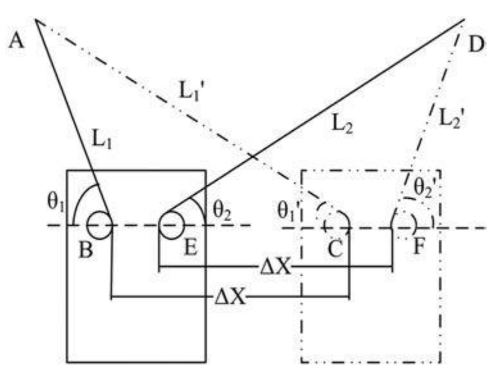

Figure 8 Moving horizontally from right to left

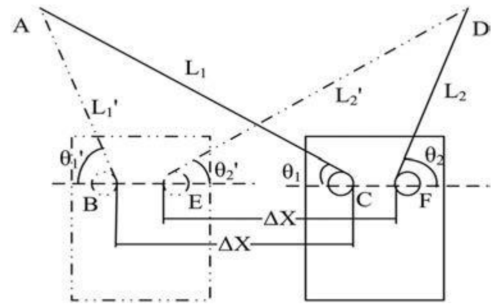

position to the line position denoted by double dots. L_1 and L_2 are the lengths of the flexible ropes before robot movement, and L'_1 and L'_2 are the lengths of the flexible ropes after robot movement. The left flexible rope driven by the left roller unreels a length of $\Delta L_1 = L'_1 - L_1$, and the right flexible rope driven by the right roller unreels a length of $\Delta L_2 = L'_2 - L_2$ (when ΔL_2 is less than zero, the right flexible rope is fully wound). Thus, the robot can move from left to right.

In $\triangle$ABC, the lengths of each sides are L'_1, L_1 and ΔX. θ_1 and θ_2 are the angles between the two flexible ropes and the oriented slider. On the basis of the law of cosines, ΔL_1 can be described as follows:

$$\Delta L_1 = \sqrt{(\Delta X)^2 + L_1^2 - 2L_1\Delta X\cos(\pi - \theta_1)} - L_1 \tag{12}$$

In a similar way, in $\triangle$DEF, ΔL_2 can be described as follows:

$$\Delta L_2 = \sqrt{(\Delta X)^2 + L_2^2 - 2L_2\Delta X\cos\theta_2} - L_2 \tag{13}$$

Figure 8 is the robot movement from right to left. ΔL_1 and ΔL_2 can be calculated as follows:

$$\begin{cases} \Delta L_1 = \sqrt{(\Delta X)^2 + L_1^2 - 2L_1\Delta X\cos\theta_1} - L_1 \\ \Delta L_2 = \sqrt{(\Delta X)^2 + L_2^2 - 2L_2\Delta X\cos(\pi - \theta_2)} - L_2 \end{cases} \tag{14}$$

5.2 Robot movement in the vertical direction

Robot movement in the vertical direction is similar to horizontal movement. The vertical movement of the robot is shown in Figure 9 and Figure 10.

Figure 9 shows the robot movement from up to down. ΔL_1 and ΔL_2 can be calculated as follows:

$$\begin{cases} \Delta L_1 = \sqrt{(\Delta Y)^2 + L_1^2 - 2L_1\Delta Y\cos(\pi/2 + \theta_1)} - L_1 \\ \Delta L_2 = \sqrt{(\Delta Y)^2 + L_2^2 - 2L_2\Delta Y\cos(\pi/2 + \theta_2)} - L_2 \end{cases} \tag{15}$$

Figure 10 shows the robot movement from down to up. ΔL_1 and ΔL_2 can be calculated as follows:

$$\begin{cases} \Delta L_1 = \sqrt{(\Delta Y)^2 + L_1^2 - 2L_1\Delta Y\cos(\pi/2 - \theta_1)} - L_1 \\ \Delta L_2 = \sqrt{(\Delta Y)^2 + L_2^2 - 2L_2\Delta Y\cos(\pi/2 - \theta_2)} - L_2 \end{cases} \tag{16}$$

Figure 9 Moving vertically from up to down

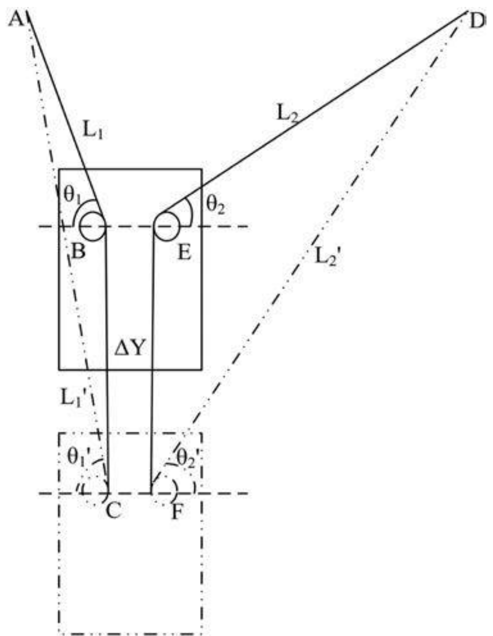

6. Force analysis of the robot with the rotor working

As shown in Figure 11, the force that the robot bears is a space force. The pressure force generated by the rotor is P, the supporting forces that the wall gives to the two supporting pieces are N_1 and N_2, the supporting force that the wall gives to the brush is N_3 and the force generated by the wind is N_4. When the rotor is working, its projection force on the XY plane is different from when the rotor is not working. Due to the existence of the angle ε between the wall and the flexible rope, F_1 and F_2 are greater when the rotor is working. At this time, the projection forces of F_1 and F_2 on the XY plane are

Figure 10 Moving vertically from down to up

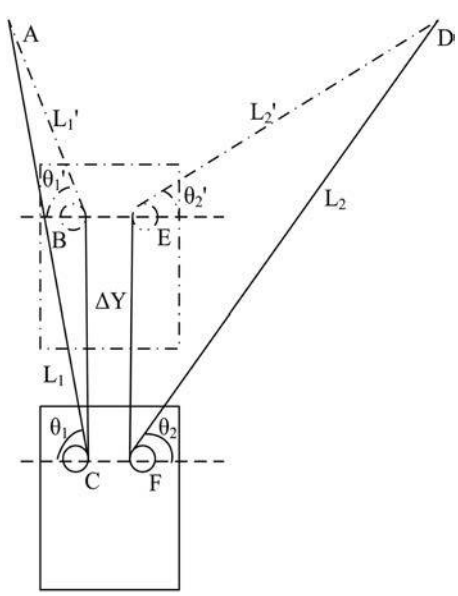

Figure 11 Space force analysis of cleaning robot

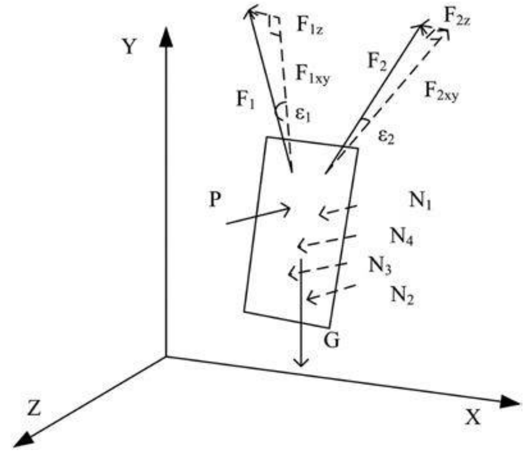

$F_{1_{xy}}$ and F_{2xy} respectively, and are equal to F_1 and F_2 when the rotor is not working. The force that the robot bears is decomposed into the forces of in the Z axis direction and in the XY plane, which are analyzed.

First, F_1 and F_2 are decomposed into the projection forces F_{1xy} and F_{2xy} on the XY plane, and F_{1z} and F_{2z}, which are paralleled with the Z axis.

$$\begin{cases} F_{1xy} = F_1 \cos \varepsilon_1 \\ F_{2xy} = F_2 \cos \varepsilon_2 \\ F_{1z} = F_1 \sin \varepsilon_1 \\ F_{2z} = F_2 \sin \varepsilon_2 \end{cases} \tag{17}$$

When the rotor is not working, the distance between the robot and the wall is b, and the length that the flexible is unreeling is L. ε can be calculated as follows:

$$\begin{cases} \varepsilon_1 = \arcsin(b/L_1) \\ \varepsilon_2 = \arcsin(b/L_2) \end{cases} \tag{18}$$

The force in the XY plane is as shown in Figure 12.

Figure 12 Force analysis in the XY plane of cleaning robot

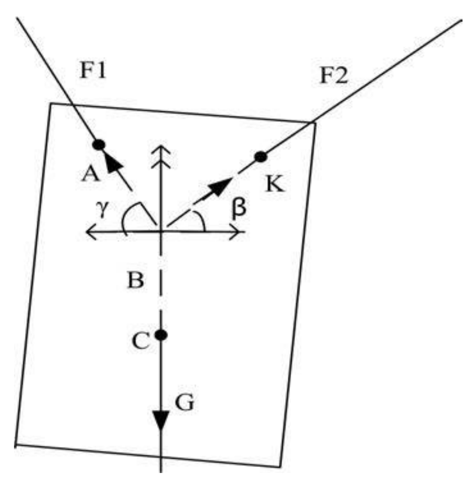

Figure 13 Experiments with robot moving along preset track: start from bottom left

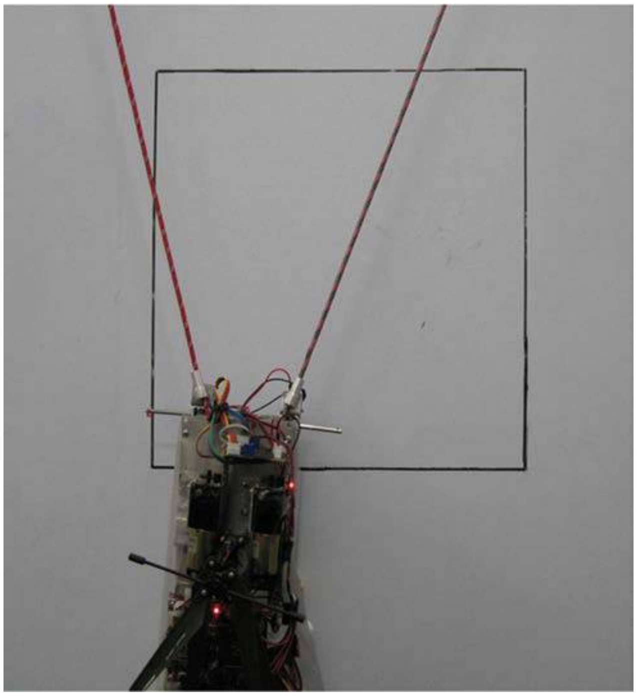

$$\begin{cases} F_{1xy}\cos\gamma = F_{2xy}\cos\beta \\ F_{1xy}\sin\gamma + F_{2xy}\sin\beta = Mg + Ma \end{cases} \tag{19}$$

where γ and β are the angles between the horizontal plane and F_{1xy} and F_{2xy}, respectively.

Because ε is very small, $\gamma \approx \theta_1 + \varphi$, and $\beta \approx \theta_2 - \varphi$, where φ is the deflection angle of the robot. Then:

$$\begin{cases} F_1 = \dfrac{Mg + Ma}{(\sin\gamma + \cos\gamma\tan\beta)\cos\varepsilon_1} \\ F_2 = \dfrac{Mg + Ma}{(\sin\beta + \cos\beta\tan\gamma)\cos\varepsilon_2} \end{cases} \tag{20}$$

In the Z axis direction:

$$P - N_1 - N_2 - N_3 - N_4 - F_{1z} - F_{2z} \tag{21}$$

N_1, N_2 and N_3 are determined by P, F_{1z} and F_{2z}. When $P = N_4 + F_{1z} + F_{2z}$, the rotor positions the robot precisely on the wall such that there is no force between the robot and the wall. If the brush exercises its cleaning function, however, it is necessary to provide a certain pressure, such that $P \geq N_4 + F_{1z} + F_{2z}$. The wind pressure formula is $P_{wind} = kv^2$, where P_{wind} is the wind pressure, v is the wind speed, k is $1/1600$. The wind speed of a fresh breeze is 8.0~10.7 m/s, and the force area of the robot is 260 mm × 110 mm, so N_4 can be calculated, and $N_4 = 2$ N. Then:

$$F_{1z} + F_{2z} = \frac{(Mg + Ma)\tan\varepsilon_1}{\sin\gamma + \cos\gamma\tan\beta} + \frac{(Mg + Ma)\tan\varepsilon_2}{\sin\beta + \cos\beta\tan\gamma} \tag{22}$$

When the robot is located at the upper-limit position of the midperpendicular of the fixed point of the two flexible ropes, $(F_{1z}+F_{2z})$ is at its maximum value. When the rotor is not working, the distance b between the robot and the wall is 20 mm, $L_1 = L_2 = 300$ mm, $\gamma = \beta = 27°$, and $F_{1z} + F_{2z} = 1.5N$. The force p provided by the rotor is measured by experiment, and is found to be $p = 4\text{N} > 3.5\text{N}$. Thus, the robot can attach to the wall reliably.

7. Control and cleaning experiment

7.1 Experiments with robot moving along preset track

To verify that the robot can move in every direction on the wall, a control experiment of the robot moving along a rectangular track is conducted. The size of the rectangular track is 390 mm × 370 mm, which is within the scope of the robot's workspace. The tracking of the robot on the rectangular track is controlled by the corresponding button on the remote control unit. The robot initially moves up along the left vertical boundary line of the rectangular track, then moves to the right along the top horizontal boundary line, then moves down along the right vertical boundary line and finally moves along the bottom horizontal boundary line to the starting point. The movement track is shown in Figure 13–16. The tracking accuracy of the robot can attain to 5 mm. The experimental result shows that tracking control of the robot along the preset track is effectively realized.

7.2 Wall cleaning experiment

To verify the cleaning function of the robot, a wall cleaning experiment is conducted. First, the robot stops at a certain position, and then the operator controls the robot to move to

Figure 14 Experiments with robot moving along preset track: to bottom right

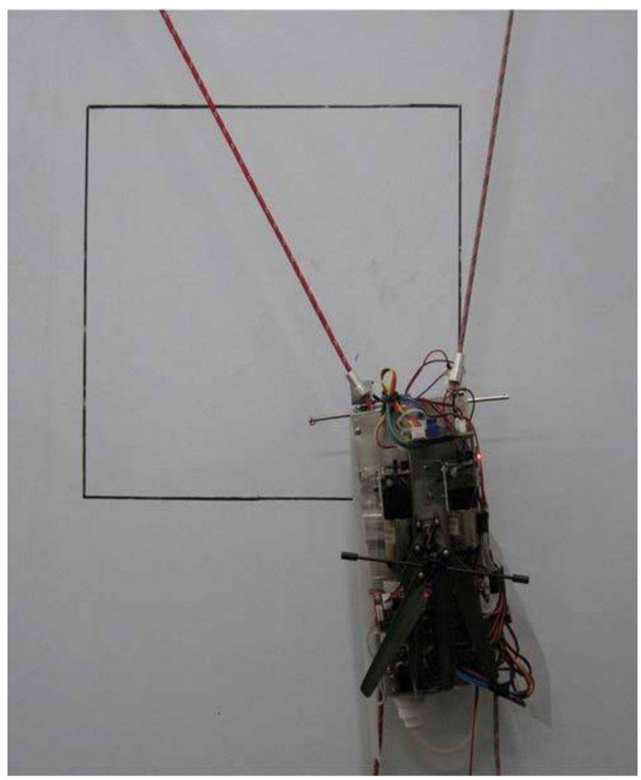

Figure 15 Experiments with robot moving along preset track: to top right

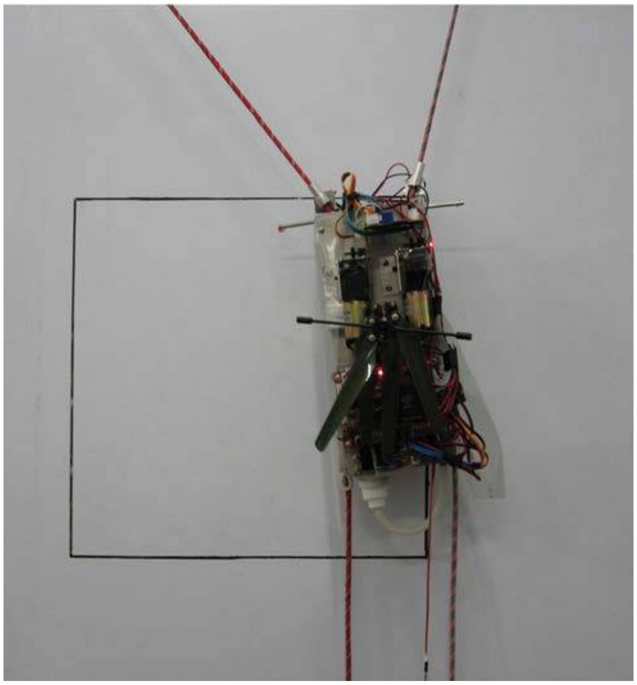

the place that needs to be cleaned. Then, the water valve is opened to spray water, and the DC motor is started so that the two brushes perform the cleaning operation. Finally, the robot finishes cleaning the dirt on the wall. The process of the cleaning experiment is shown in Figure 17 and 18.

Figure 16 Experiments with robot moving along preset track: to top left

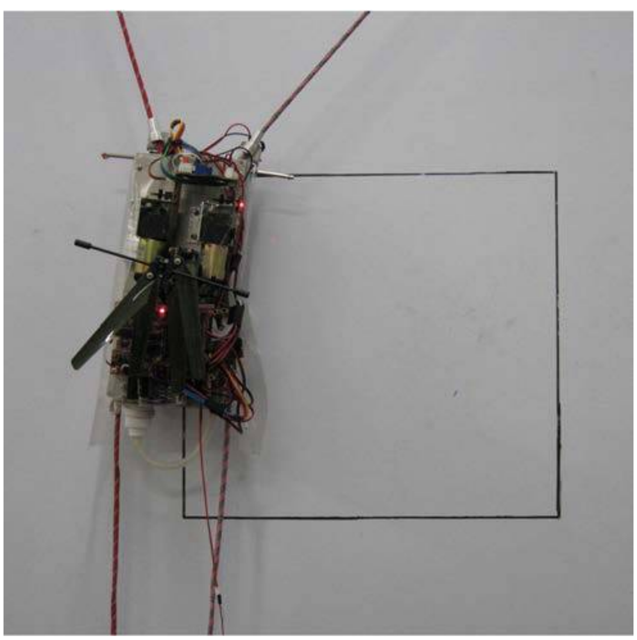

Figure 17 Process of the cleaning experiment: close to the clean areas

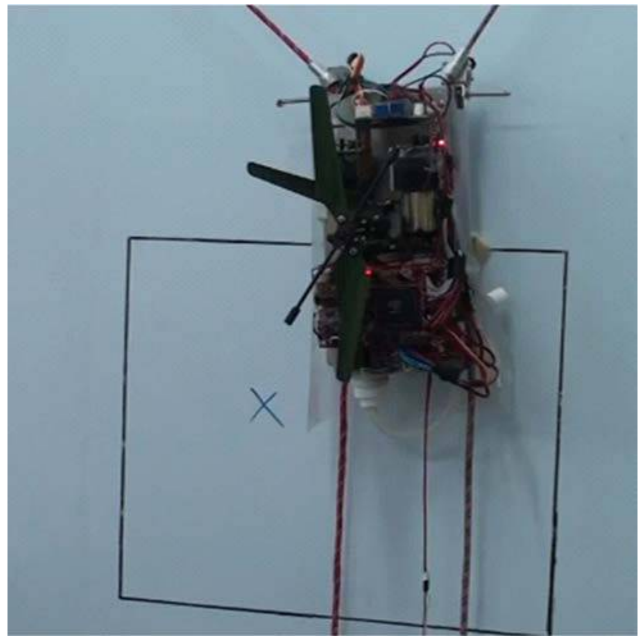

8. Conclusion

The glass curtain wall, because of its excellent daylighting performance, damp-proofing characteristics, heat insulation properties and aesthetics, is widely used in modern city buildings. For glass-curtain-wall buildings, regular cleaning of the glass curtain wall is necessary to ensure that the surface of

Figure 18 Process of the cleaning experiment: spraying water and brushing

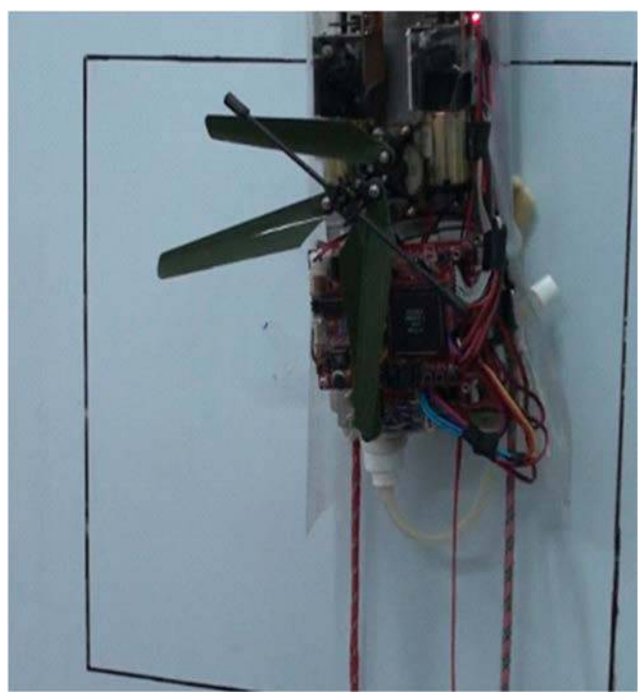

the building appears clean and tidy, which in turn contributes toward preserving the overall aesthetic appearance of the city. Currently, the primary method of glass-curtain-wall cleaning is manual cleaning by workers on a suspended platform. This method is totally dependent on manual work and suffers from shortcomings such as high labor intensity, low efficiency and high risk. A glass-curtain-wall cleaning robot driven by a double flexible rope is developed based on inspiration from spiders that move in the air by pulling their silk draglines. A worm reducer is designed to realize the self-locking protection function. A multislot master-slave roller in the moving section increases the flexible rope friction. The cleaning section consists of a water tank, control valve, sprayer and cleaning brush. The absorbing section, realized by a rotor, is also designed. The workspace of the robot, control analysis of winding and unreeling, analysis of the flexible rope and force analysis of the robot are conducted. Based on a prototype of a glass-curtain-wall cleaning robot driven by flexible ropes, experiments wherein the robot moves along a preset track, as well as cleaning experiments, are performed. The robot satisfies the design functions and cleans effectively. The experimental results verify the validity and practicality of the robot. Traditional manual cleaning by workers on a suspended platform will be changed after the glass-curtain-wall cleaning robot is manufactured, and the advent of cleaning robots for low- and mid-rise buildings will reduce the cost of building cleaning, improve the working environment and enhance production efficiency.

References

Akinfiev, T., Armada, M. and Nabulsi, S. (2009), "Climbing cleaning robot for vertical surfaces", *Industrial Robot: An International Journal*, Vol. 36 No. 4, pp. 352-357.

Chen, I.M. and Yeo, S.H. (2003), "Locomotion of a two-dimensional walking-climbing robot using a closed-loop mechanism: from gait generation to navigation", *The International Journal of Robotics Research*, Vol. 22 No. 1, pp. 21-40.

Chu, B., Jung, K., Han, C.S. and Hong, D. (2010), "A survey of climbing robots: locomotion and adhesion", *International Journal of Precision Engineering and Manufacturing*, Vol. 11 No. 4, pp. 633-647.

Guan, Y.S., Zhu, H.F., Wu, W.Q., Zhou, X.F., Jiang, L., Cai, C.W., Zhang, L.M. and Zhang, H. (2013), "A modular biped wall-climbing robot with high mobility and manipulating function", *IEEE-ASME Transactions on Mechatronics*, Vol. 18 No. 6, pp. 1787-1798.

Guido, L.R., Michele, M. and Giovanni, M. (2002), "A low-cost lightweight climbing robot for the inspection of vertical surfaces", *Mechatronics*, Vol. 12 No. 1, pp. 71-96.

He, B., Wang, Z.P., Li, M.H., Wang, K., Shen, R.J. and Hu, S.Q. (2014), "Wet adhesion inspired bionic climbing robot", *IEEE-ASME Transactions on Mechatronics*, Vol. 19 No. 1, pp. 312-320.

Hirai, M., Hirose, S. and Lee, W. (2013), "Gunryu III: reconfigurable magnetic wall-climbing robot for decommissioning of nuclear reactor", *Advanced Robotics*, Vol. 27 No. 14, pp. 1099-1111.

Hu, B.S., Wang, L.W., Zhao, Y.Z. and Fu, Z. (2009), "A miniature wall climbing robot with biomechanical suction cups", *Industrial Robot: An International Journal*, Vol. 36 No. 6, pp. 551-561.

Hwang, K., Dongmok, K. and Hojoon, Y. (2008), "Development of a wall-climbing robot using a tracked wheel mechanism", *Journal of Mechanical Science and Technology*, Vol. 22 No. 8, pp. 1490-1498.

Jaradat, M.A.K., Ashour, S.M., Matalkh, A.A., Elayyan, M.M. and Hammadneh, A.M. (2010), "Biologically inspired design of a glass climbing robot for remote services", *International Journal of Robotics and Automation*, Vol. 25 No. 2, pp. 132-141.

Kalra, L.P. and Gu, J. (2007), "An autonomous self contained wall climbing robot for non-destructive inspection of above-ground storage tanks", *Industrial Robot: An International Journal*, Vol. 34 No. 2, pp. 122-127.

Koo, I.M., Trong, T.D., Lee, Y.H., Moon, H., Koo, J., Park, S.K. and Choi, H.R. (2013), "Development of wall climbing robot system by using impeller type adhesion mechanism", *Journal of Intelligent and Robotic Systems*, Vol. 72 No. 1, pp. 57-72.

Lee, G., Wu, G., Kim, J. and Seo, T. (2012), "High-payload climbing and transitioning by compliant locomotion with magnetic adhesion", *Robotics and Autonomous Systems*, Vol. 60 No. 10, pp. 1308-1316.

Liu, J.H., Tanaka, K., Bao, L.M. and Yamaura, I. (2006), "Analytical modelling of suction cups used for window-cleaning robots", *Vacuum*, Vol. 80 No. 6, pp. 593-598.

Menon, C. and Metin, S. (2006), "A biomimetic climbing robot based on the Gecko," *Journal of Bionic Engineering*, Vol. 3 No. 3, pp. 115-125.

Qian, Z.Y., Fu, Z. and Liu, R.Q. (2006), "Analysis of the adaptability of cleaning robot to glass-curtain wall surface", *Journal of Shanghai Jiaotong university*, Vol. 40 No. 7, pp. 1157-1165.

Qian, Z.Y., Zhao, Y.Z. and Fu, Z. (2006), "Design and realization of a non-actuated glass-curtain wall-cleaning robot prototype with dual suction cups", *The International Journal of Advanced Manufacturing Technology*, Vol. 30 Nos 1/2, pp. 147-155.

Sameoto, D., Li, Y.S. and Menon, C. (2008), "Multi-scale compliant foot designs and fabrication for use with a spider-inspired climbing robot", *Journal of Bionic Engineering*, Vol. 5 No. 3, pp. 189-196.

Schmidt, D. and Berns, K. (2013), "Climbing robots for maintenance and inspections of vertical structures: a survey of design aspects and technologies", *Robotics and Autonomous Systems*, Vol. 61 No. 12, pp. 1288-1305.

Sun, D., Zhu, J., Lai, C.M. and Shiu-Kit, T. (2004), "A visual sensing application to a climbing cleaning robot on the glass surface", *Mechatronics*, Vol. 14 No. 10, pp. 1089-1104.

Suzuki, K., Nemoto, S., Fukuda, T., Takanobu, H. and Miura, H. (2010), "Insect-inspired wall-climbing robots utilizing surface tension forces", *Journal of Advanced Mechanical Design Systems and Manufacturing*, Vol. 4 No. 1, pp. 383-390.

Tavakoli, M., Viegas, C., Marques, L. and De Almeida, A.T. (2013), "OmniClimbers: omni-directional magnetic wheeled climbing robots for inspection of ferromagnetic structures", *Robotics and Autonomous Systems*, Vol. 61 No. 9, pp. 997-1007.

Wang, W., Tang, B.Y., Zhang, H.X. and Zong, G.H. (2010), "Robotic cleaning system for glass facade of high-rise airport control tower", *Industrial Robot: An International Journal*, Vol. 37 No. 5, pp. 469-478.

Xu, G.H., Liu, Z.R. and Zhong, X.Q. (2011), "Research on a new glass-curtain cleaning robot", *2011 International Conference on Consumer Electronics, Communications and Networks*, XianNing, pp. 4330-4333.

Yu, Z.W., Gong, J. and Zhang, H. (2011), "One-leg motion control of gecko robot based on three-dimensional force feedback", *Chinese Journal of Scientific Instrument*, Vol. 32 No. 12, pp. 2674-2678.

Zhang, H.X., Zhang, J.W. and Zong, G.H. (2006), "Sky Cleaner 3: a real pneumatic climbing robot for glass-wall cleaning," *IEEE Robotics and Automation Magazine*, Vol. 13 No. 1, pp. 32-41.

Zhang, Y. and Wang, Y.N. (2010), "Odd Gabor edge detection algorithm for condenser cleaning robot," *Chinese Journal of Scientific Instrument*, Vol. 31 No. 10, pp. 1564-1568.

Zhao, Y.Z., Fu, Z. and Cao, Q.X. (2004), "Development and applications of wall-climbing robots with a single suction cup", *Robotica*, Vol. 22 No. 6, pp. 643-648.

Zhu, J., Sun, D. and Shiu-Kit, T. (2002), "Development of a tracked climbing robot", *Journal of Intelligent and Robotic Systems*, Vol. 35 No. 4, pp. 427-443.

Zhu, J., Sun, D. and Shiu-Kit, T. (2003), "Application of a service climbing robot with motion planning and visual sensing", *Journal of Robotic Systems*, Vol. 20 No. 4, pp. 189-199.

Corresponding author

Jiang Jin-gang can be contacted at: jiangjingang@hrbust.edu.cn